PHOTOELASTIC ANALYSIS OF THE MAXIMUM STRESS IN A PLATE WITH A REINFORCED CIRCULAR HOLE UNDER UNIAXIAL TENSION

MASAICHIRŌ SEIKA

Department of Mechanical Engineering

(Received September 22, 1967)

ABSTRACT

In this paper, the author compiled his study on the reinforcing ring which was published in parts in the Transactions of the Japan Society of Mechanical Engineers and other periodicals during the last several years[1)~7)].

The photoelastic stress-freezing method is applied to determine the stress concentrations around circular holes in flat plates, reinforced by rings with fillets which are symmetrically placed with respect to the plates, under uniaxial tension. The investigation is performed on the rings of different proportions and on the fillets of various radii of curvature, and the three dimensional effects of reinforcements on the stress concentrations around the circular holes are examined. Both the effective height of the reinforcing ring and the minimum radius of curvature of the fillet effective in reducing the stress concentration in a perforated plate are studied in connection with the optimum reinforcement.

Introduction

The stress concentrations produced by circular holes occurring in machine parts or structural members under various loads are frequently reduced by means of reinforcing rings. Accordingly, it is of practical importance to obtain the dimensions of rings for the optimum reinforcement. A number of theoretical analyses have been made on this subject[8)~14)] in which, however, the stresses in reinforcing rings are assumed to be in a state of plane stress; namely, the stresses are assumed to distribute uniformly along the whole height of the ring. The two-dimensional assumption differs apparently from the actual state and leads to erroneous conclusions when the height of reinforcing rings is larger than the thickness of plates. The stresses in reinforcing rings should be analyzed by the three-dimensional approach. In experimental studies, however, the problem has been investigated three-dimensionally. The peak strain in a reinforcing ring under various biaxial tension fields was measured by the use of foil strain gages[15)]. A photoelastic investigation of a symmetrical reinforcing ring was also made by Suzuki[16)] by applying the laminated layers method. In those studies, however, the investigation for a reinforcement only in a wide plate is performed. It is of practical interest to examine the effect of the edges on the maximum stress at the rim of a reinforced hole for finite plates. Moreover, in those ex-

perimental studies, the problem of a reinforcing ring without fillets is treated, while the reinforcing rings with fillets are frequently used in practice. It can easily be inferred that the fillets of the reinforcing ring reduce not only the stress concentration in the plate near the reinforcement but also the maximum stress at the edge of the hole.

In the present paper, the photoelastic stress-freezing and slicing technique was applied to obtain the maximum stress at the edge of a circular hole in a plate reinforced with a symmetrical reinforcing ring with fillets, under uniaxial tension. Furthermore, the stress concentration in the plate at the corners of fillets was examined. Test models were made of epoxy resin, and were fabricated by attaching the reinforcing ring to the plate or by casting the model so as to make the ring and plate one body. The investigation was performed on different widths of the plate and various dimensions of the ring with fillets. From the results herein obtained, the effective height of the reinforcing ring effective in reducing the maximum stress at the edge of the hole was studied in connection with the optimum reinforcement. Moreover, as a result of measurement of the stress concentrations at the ends of fillets, the minimum radius of curvature of the fillet was examined, which effectively increases the strength of the plate near the reinforcement.

Experimental Procedure

Test Models—The test model used was made of epoxy resin, and consisted of a nominally 6-mm-thick plate and a symmetrical reinforcing ring with fillets having an outer diameter of 30-mm, which was kept constant, as shown in Fig. 1. It was fabricated by attaching the reinforcing ring to the inside of a central circular hole cut in the plate by the use of an adhesive, namely, Eastman 910. The cemented location between the plate and the ring was taken a little outer side from the end of the fillet. For an accurate measurement of the stress concentration at the end of the fillet, even a slight disorder of the stress distribution in the plate near the fillet-end arising from the cementation should be avoided. Accordingly, the models used in such experiments were produced by casting so as to make the ring and plate one body, using a mold of poly-tetrafluoroethylene. Special precaution was taken for machining the circular fillets with accurate profiles, so the radii of curvature at the tip of cutting tool were carefully examined so as to have the prescribed dimensions. In order to distribute the applied load as evenly as possible, the plate was pin-loaded through several holes at both ends by means of

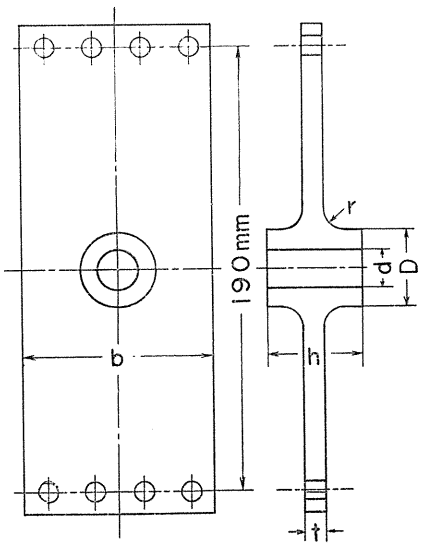

FIG. 1. Test model.

TABLE 1. Nominal Dimensions of Test Models

t mm	b mm	D mm	d mm	h mm	r mm	d/D	h/t	r/t
6	30 45 60 120	30	9 15 21	6 12 18 24 30	0 1 2 3.5 5 10	0.3 0.5 0.7	1 2 3 4 5	0 0.17 0.33 0.58 0.83 1.67

a dead weight, the loading device being adjusted minutely at both the top and bottom connections. The plate was sufficient in length so that the stress, applied across the section adjacent to the ring, might hold substantially uniform distribution. Nominal dimensions of the parts of the models examined are shown in Table 1.

Stress-Freezing Technique—In carrying out the freezing procedure, the test models were heat treated and observed, in a temperature controlled oven. Since the oven is equipped with a fan to provide the effective circulation of hot air, the temperature distribution in the vicinity of the test model can be evenly kept within $\pm 1°C$. Figure 2 shows the oven containing a model under the freezing procedure. The stress-freezing cycle employed consisted of the following stages: The temperature in the oven containing an unloaded model was raised to 130°C, which was the temperature above the transition-temperature of the material used, and the temperature was kept constant for about one hour. In this stage, the initial stresses in the model due to machining could be eliminated, although in the models produced by cementation a small amount of the residual stress was

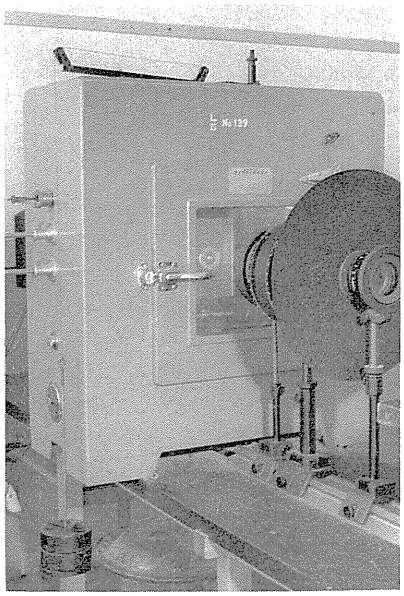

FIG. 2. Oven containing a model under freezing procedure.

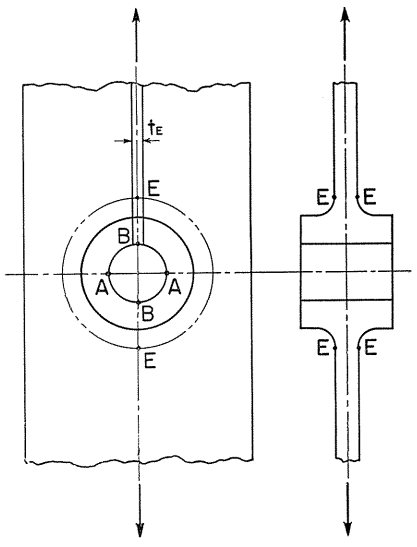

FIG. 3. Locations producing stress concentration.

observed at the bonded interface of the plate and ring. Next, the load was applied to the specimen. To equilibrate the stresses produced in the model, the temperature was kept constant for about one hour, and then cooled at a constant rate of 5°C per hour. When the temperature fell to room temperature the load was removed, and the model was sliced, and the examination for the fringe order was made at the measuring points by the use of a conventionally arranged polariscope.

Maximum Stress in the Reinforcing Ring—The maximum stress in the ring arises at the location A, shown in Fig. 3. In general, the relation between the fringe order n and the principal stress σ, kg/mm², at the free boundary is given by the expression

$$n = \alpha\sigma S, \tag{1}$$

where α is the photoelastic sensitivity of material, mm/kg, at the temperature for freezing the stresses, and S is the thickness of slices, mm. The fringe orders n_1 and n_2 at the location A were successively measured, in which n_1 was the fringe order for the whole height of the ring, h, and n_2 for the height sliced off to the plate thickness t. These fringe orders were taken as the averaged value at the location A on both sides of the hole. To obtain the fractional order of the fringe, the Tardy method was applied. In reducing practically the height of the ring to the plate thickness, the model was clamped solidly to the face plate of a lathe and the material was lightly cut out from the model by supplying a plenty of cutting oil. However, since the cast model was used again for the measurement of the fringes at the end of the fillet, only the material around the hole was cut out from the ring, leaving the material around the fillet-end. Using Equation (1), the mean stress through the thickness at the location A for each height of the ring is expressed as

$$\sigma_1 = \frac{n_1}{\alpha h}, \qquad \sigma_2 = \frac{n_2}{\alpha t}. \tag{2}$$

The stress-concentration factor is then defined by the following formulae:

$$K_1 = \frac{\sigma_1}{\sigma_0}, \qquad K_2 = \frac{\sigma_2}{\sigma_0}, \tag{3}$$

where σ_0 is the nominal stress based on the gross section of the plate.

At the temperature 130°C, the Young's modulus of the material reduces remarkably. Accordingly, in order to avoid the error arising from the deformation of specimens, the applied load was limited so as to keep the fringe order n_2 about three. In this case, the maximum difference in the inner diameters of the ring at right angle was within one per cent, so the effect on the experimental results was not perceptible.

For calibrating the photoelastic sensitivity α of the material at 130°C, circular plates diametrically compressed were employed under the same stress-freezing cycle described in the foregoing. The averaged value of α, which was measured for every test model, was 41 mm/kg (λ=5461 Å).

Stress Concentration at the End of the Fillet—The investigation was performed only for a tension plate having finite width, namely, $b/D=2$. The maximum stress at the end of the fillet occurs at the location E on the axis of the model, as shown in Fig. 3. The slice containing the location E. which was of about 2.5 mm in thickness, was cut out in parallel with the axis of the model. The fringe order at the location E, n_E, which was taken as the averaged value at four locations, was obtained. The mean stress σ_E for the thickness of the slice at the location E, t_E, is given from Equation (1) as

$$\sigma_E = \frac{n_E}{\alpha t_E}. \tag{4}$$

Accordingly, the stress-concentration factor at the end of the fillet, K_E, is expressed by the formula

$$K_E = \frac{\sigma_E}{\sigma_0}. \tag{5}$$

Influence of Cementation—It is essential to examine the influence of cementation between the ring and the plate, on the stress distribution in the ring. The stress distribution in the model cemented with a ring of $h/t=1$ was compared with that in a tension plate of the same width, containing a circular hole of the same diameter, under the same stress-freezing cycle and load. As an example, dark-field frozen-stress patterns are shown in Figs. 4 (a), (b) and 5 (a), (b). As is

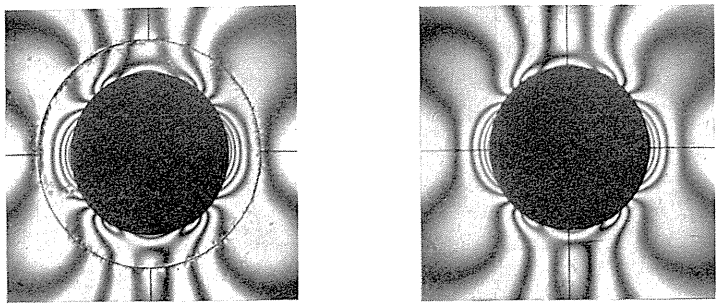

(a) $d/D=0.7$ (b)

FIG. 4. Dark-field frozen-stress patterns for $h/t=1$.

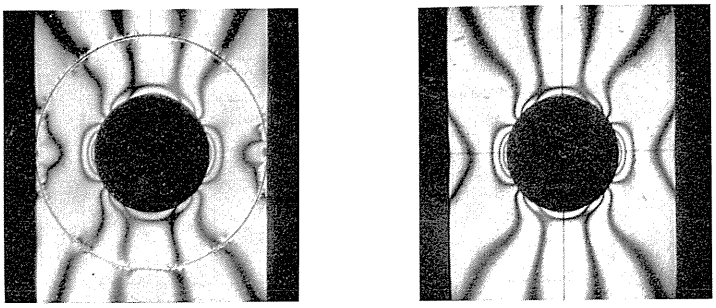

(a) $d/D=0.5$ (b)

FIG. 5. Dark-field frozen-stress patterns for $h/t=1$.

shown in the figures, the continuity of the stress pattern is not disturbed over the plate and ring, and the stress patterns of the two cases are in excellent agreement except the vicinity of the cemented portion. Accordingly, the effect of cementation on the stresses at the inner surface of the reinforced hole can be ignored.

Experimental Results and Discussion

Wide Plates—The experiments were performed on the models with wide plates, namely, $b/D=4$. The nominal dimensions of the rings were: $d/D=0.3$, 0.5, 0.7, $h/t=1\sim5$, and $r/t=0$, 0.33, 0.58, 0.83.

If the width of a plate having a central circular hole is not less than four diameters of the hole, the edges of the plate have little effect on the maximum stress occurring at the rim of the hole[17]. Since the width of the wide plate examined is four times as large as the outer diameter of the ring, the results herein obtained may be approximated to those of an infinite plate.

Figure 6 shows magnified profiles of the fillets of various radii of curvature.

The stress-concentration factors K at the location A (Fig. 3) for each value of r/t, plotted as a function of h/t, are shown in Figs. 7, 8, 9 and 10. In Fig. 7,

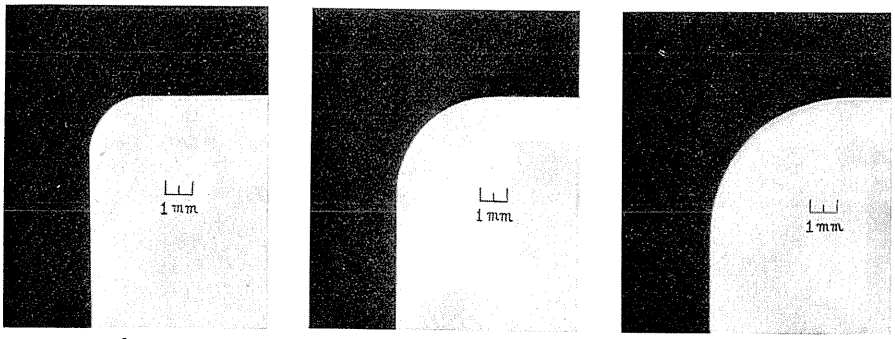

$r=2$ mm $r=3.5$ mm $r=5$ mm

FIG. 6. Magnified profiles of fillets.

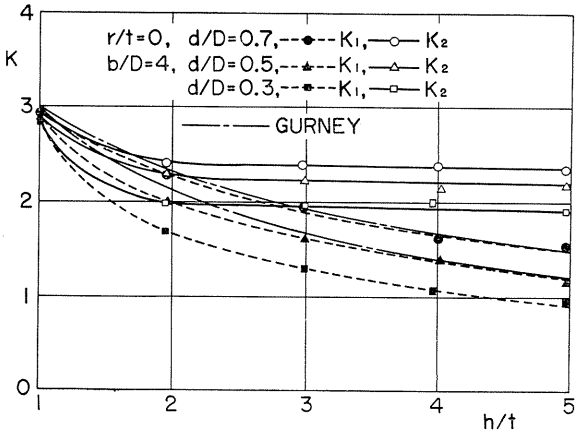

FIG. 7. Stress-concentration factor K for $r/t=0$ and $b/D=4$.

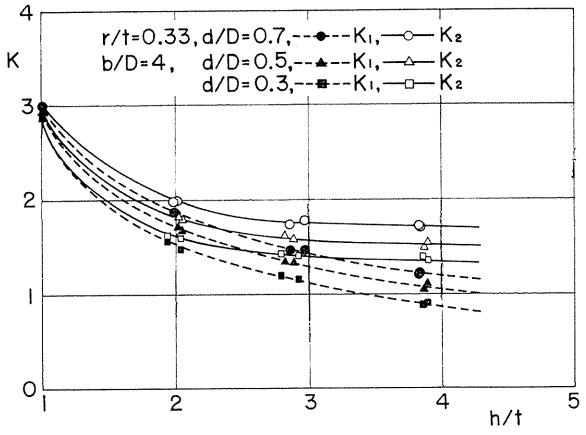

FIG. 8. Stress-concentration factor K for $r/t=0.33$ and $b/D=4$.

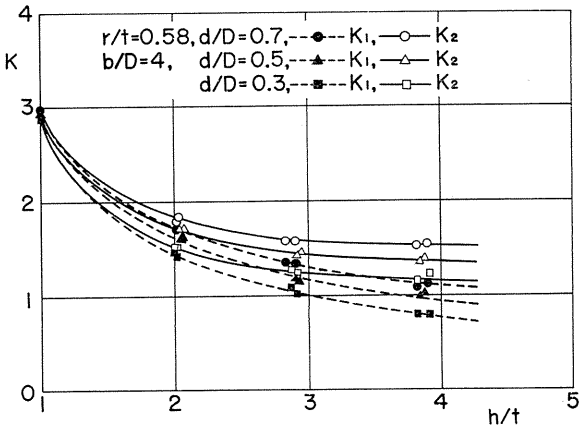

FIG. 9. Stress-concentration factor K for $r/t=0.58$ and $b/D=4$.

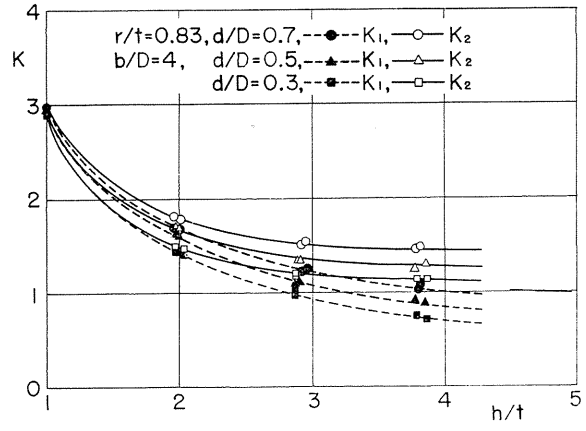

FIG. 10. Stress-concentration factor K for $r/t=0.83$ and $b/D=4$.

the values of K_1 are shown together with the theoretical results obtained by Gurney[8] for $d/D=0.5$ and 0.7. These are the values based on the assumption that the stresses do not vary through the height of the ring. The agreement between the experimental and theoretical values is satisfactory. Inspection of the curves in these figures shows that the factor K_2, which was obtained by slicing off the ring to the plate thickness, becomes much larger than K_1 with increase of h/t and becomes almost constant for $h/t>3$. This indicates that the limit of the effective height of a reinforcing ring in a wide plate is three times as large as the plate thickness.

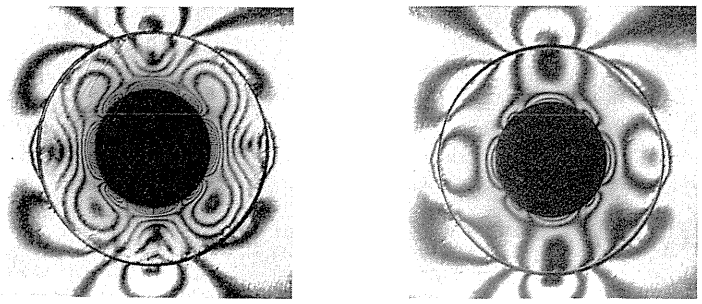

$K_1=1.60$ $K_2=2.24$

$h/t=2.98,\ d/D=0.5,\ r/t=0$

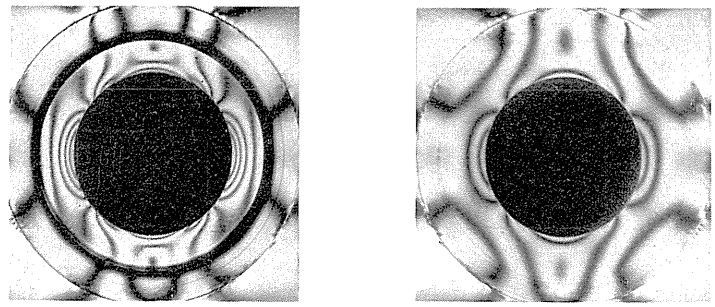

$K_1=1.85$ $K_2=1.99$

$h/t=2.02,\ d/D=0.7,\ r/t=0.33$

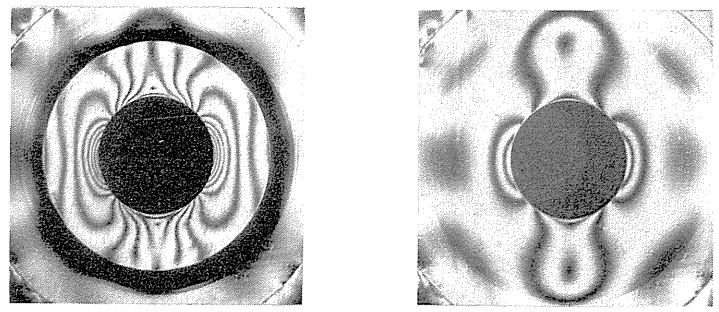

$K_1=1.16$ $K_2=1.46$

$h/t=2.94,\ d/D=0.5,\ r/t=0.58$

FIG. 11. Dark-field frozen-stress patterns in rings ($b/D=4$).

From the further examinations on the maximum stress at the location A, by using the slices about 3-mm-thick cut symmetrically with respect to the middle plane of plates, it was found that the actual maximum stress occurring at the midpoint of the height of rings was somewhat larger than σ_2.

Figure 11 shows the typical dark-field frozen-stress patterns in the rings before and after slicing.

From the results thus obtained, the relation between the stress-concentration factor and the radius of curvature of the fillet is represented in Figs. 12, 13 and 14, where the factors K for each value of h/t are plotted as a function of r/t. As shown in the figures, when a reinforcing ring is provided with fillets, the factors K are reduced markedly with increase of r/t and this tendency is notable with increase of h/t. Moreover, when $r/t>0.6$, the factors K become almost constant for every height of the rings examined. This indicates that the limit of the effective radius of curvature of the fillet is 0.6 times as large as the plate thickness. If the dimensions of the reinforcing ring are chosen as $h/t=3$ and $r/t=0.6$ for each wall thickness, the factors K_2 are about 35 per cent smaller than those of the filletless ring, as is shown in Fig. 13.

At the location B in Fig. 3, the maximum stress in compression occurs. When the maximum stress at the location B obtained by slicing off the ring to the plate thickness is expressed by the stress-concentration factor K_2', for instance, the factors K_2' for $r/t=0.58$ are shown in Fig. 15. Combining the values of K_2 in Fig. 9 with those of K_2' in Fig. 15, the stress-concentration factors at the edge of the reinforced hole can be obtained for the case when a wide plate is subjected

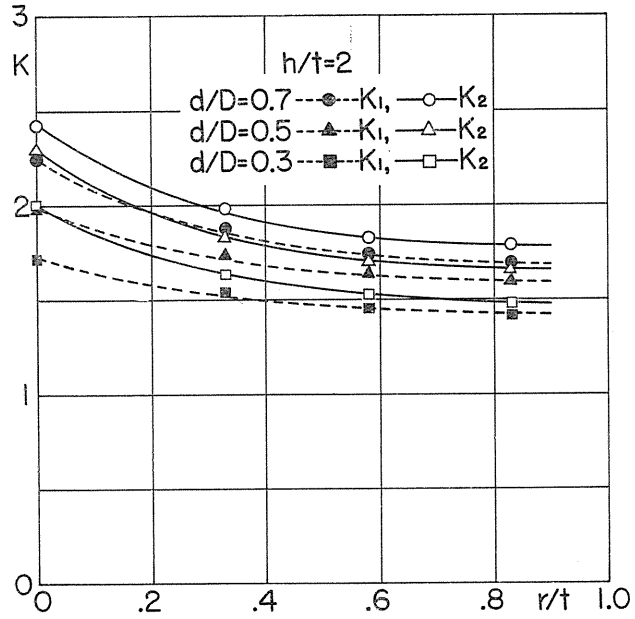

FIG. 12. Stress-concentration factor K for $h/t=2$ and $b/D=4$.

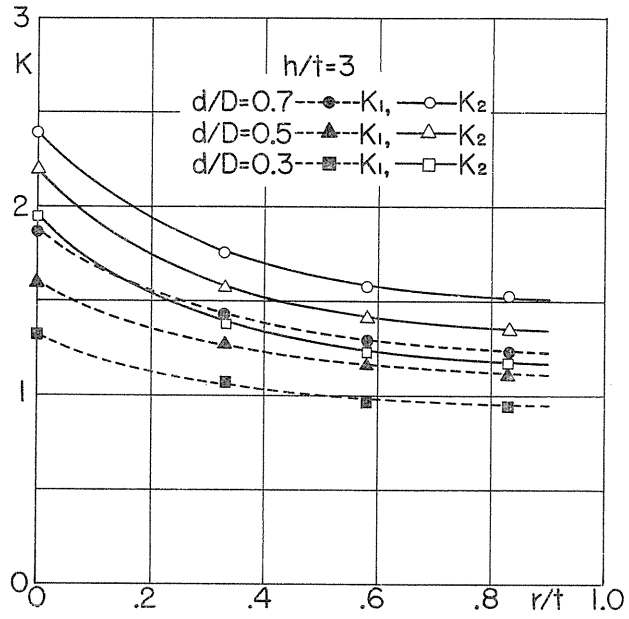

FIG. 12. Stress-concentration factor K for $h/t=3$ and $b/D=4$.

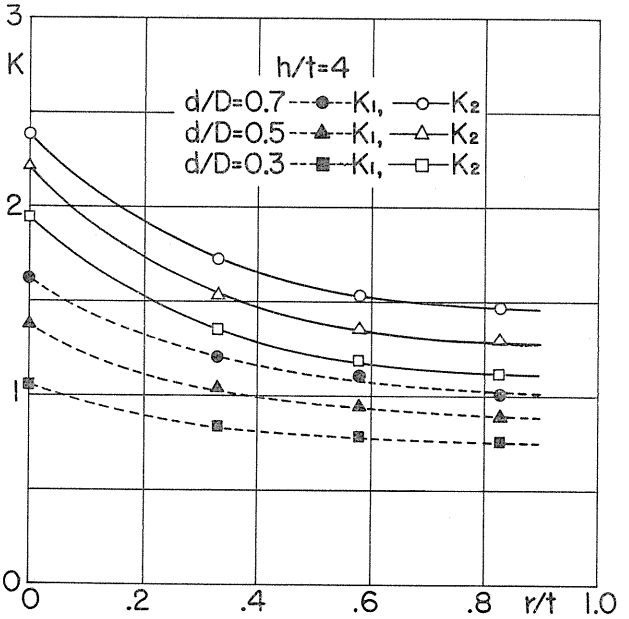

FIG. 14. Stress-concentration factor K for $h/t=4$ and $b/D=4$.

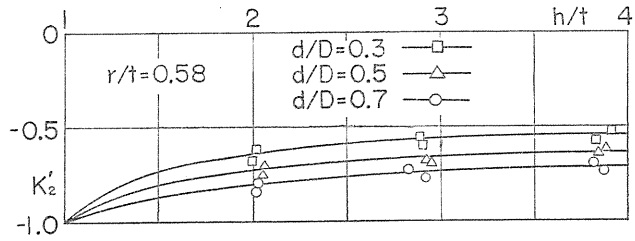

FIG. 15. Stress-concentration factor K_2' for $r/t=0.58$ and $b/D=4$.

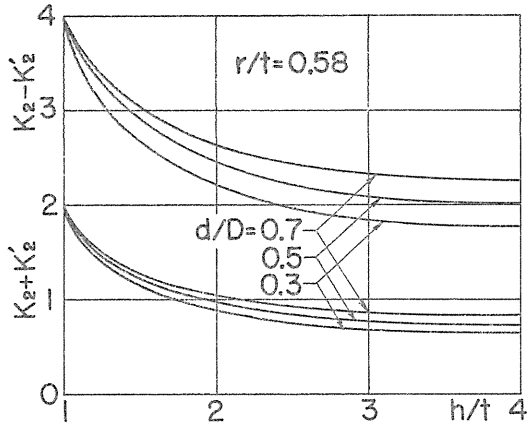

FIG. 16. Stress-concentration factors $K_2 \pm K_2'$ for $r/t=0.58$ and $b/D=4$.

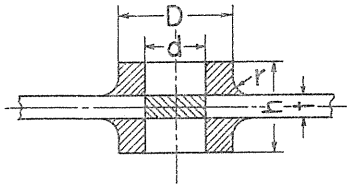

FIG. 17. Section of reinforcement.

to biaxial tension. Figure 16 shows the relation between the stress-concentration factors and the height of the ring, h/t, in which the ordinates K_2+K_2' and K_2-K_2' express the stress-concentration factors in biaxial tension of the same magnitude and pure shear, respectively. As shown in the figure, these factors are reduced markedly with increase of h/t and become almost constant for $h/t>3$ in either case.

Practically, the stress-concentration factor K_2 is often represented as a function of the relative weight of the reinforcing ring, v, namely, the ratio of the volume of the ring to that of the hole. From Fig. 17, the volume of the ring, V, is given as

$$V=\frac{\pi}{4}\left[(h-t)(D^2-d^2)+(8-2\pi)Dr^2+\left(\frac{40}{3}-4\pi\right)r^3\right]. \tag{6}$$

Accordingly, the relative weight v is expressed by the following formula:

$$v = \frac{(h-t)(D^2-d^2)+1.72\,Dr^2+0.77\,r^3}{d^2t}. \tag{7}$$

The curves of the factor K_2 for the heights $h/t=3$ and 4 of the ring, plotted as a function of v, are shown in Fig. 18. As shown in the figure, the difference between the factor K_2 of $r/t=0.58$ and that of $r/t=0.83$ is small. Hence, it can easily be seen that the effective minimum of r/t is 0.6, as was mentioned in the foregoing. Inspection of the curves shows that when $v>20$, the factors K_2 reduce very gradually. This indicates that the effective maximum of the relative weight v is 20. From Fig. 18 and Equation (7), one can find the optimum wall thickness of the reinforcing ring, D/d, provided that the ratio of the hole diameter to the plate thickness, d/t, is given. As an example, when $h/t=3$ and $r/t=0.6$, the relations between d/t and D/d for $v=10$ and 20 are shown in Table 2, respectively.

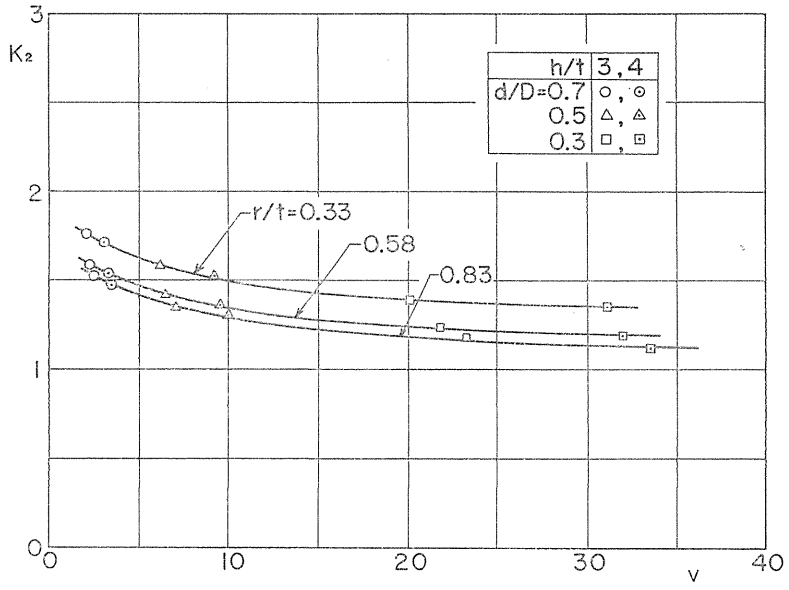

FIG. 18. Stress-concentration factor K_2, as function of relative weight v, for $h/t=3$ and 4.

TABLE 2. Relations between d/t and D/d ($h/t=3$, $r/t=0.6$)

$v=10$: $K_2=1.32$						
d/t	0.5	1	2	5	10	∞
D/d	2.09	2.28	2.36	2.42	2.43	2.45
$v=20$: $K_2=1.22$						
d/t	0.5	1	2	5	10	∞
D/d	2.97	3.15	3.24	3.29	3.30	3.32

Finite Plates—In order to examine the edge effect of the tension plates on the maximum stress at the rim of a reinforced hole, the experiments were carried out in the range of the plate width from D up to $2D$, namely, $b/D=1$, 1.5 and 2. The dimensions of the rings tested were taken as $d/D=0.3$, 0.5, 0.7, and $h/t=1\sim5$ as in the preceding examples, and the radii of curvature of the fillets, r/t, were varied from 0 up to 1.67. For the purpose of an accurate measurement of the stress concentration at the ends of the fillets, the test models with tension plates

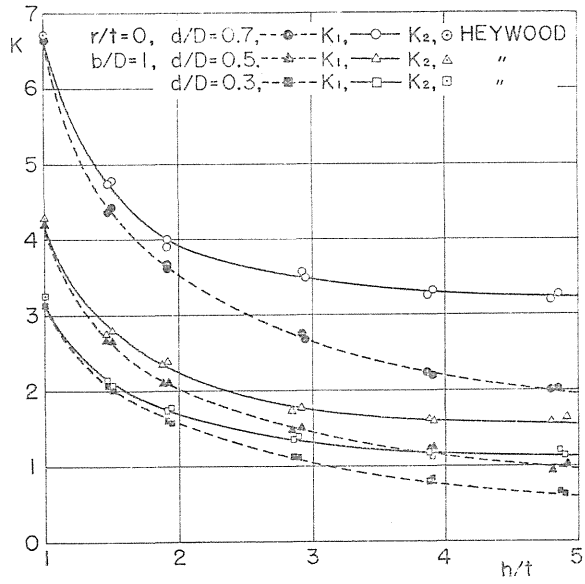

FIG. 19. Stress-concentration factor K for $r/t=0$ and $b/D=1$.

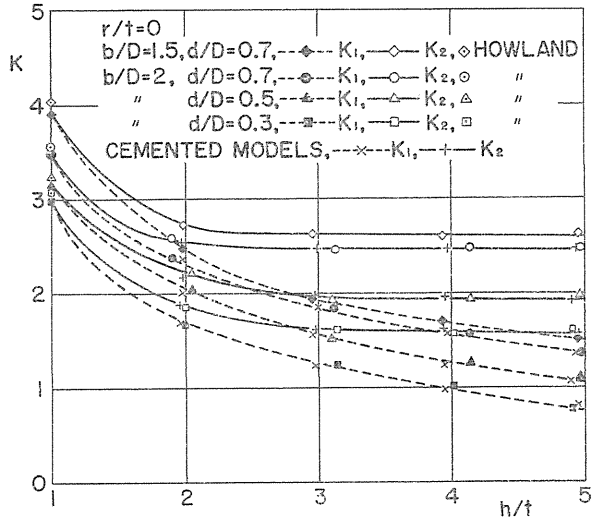

FIG. 20. Stress-concentration factor K for $r/t=0$, and $b/D=1.5$ and 2.

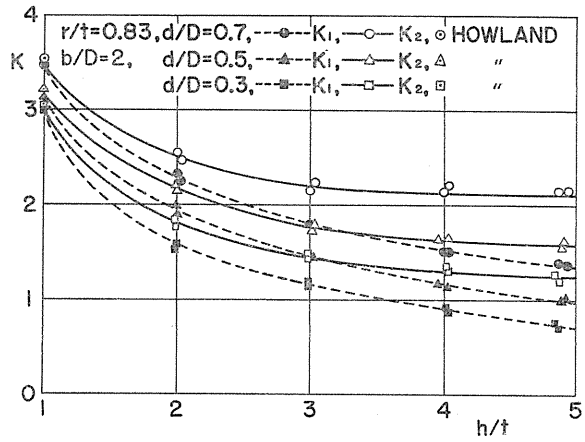

FIG. 21. Stress-concentration factor K for $r/t=0.83$ and $b/D=2$.

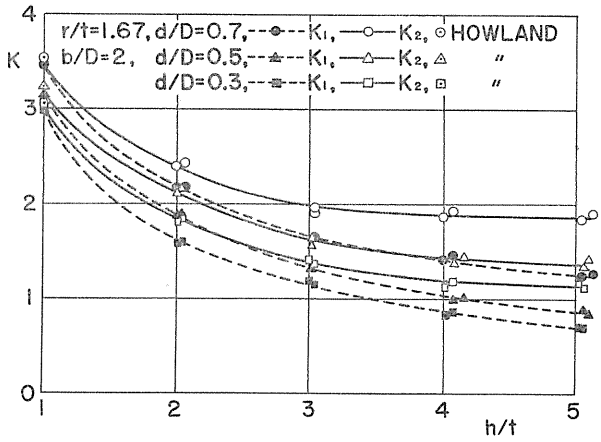

FIG. 22. Stress-concentration factor K for $r/t=1.67$ and $b/D=2$.

of $b/D=2$ were produced by casting so as to make the reinforcing ring and the plate in one body.

The stress-concentration factor K at the location A (Fig. 3) for various values of b/D and r/t, plotted as a function of h/t, are shown in Figs. 19, 20, 21 and 22. In these figures, symbols ◈, ⊙, ◬ and ◙ at $h/t=1$ are the theoretical values given by Howland[18] and the values calculated by Heywood's empirical formula[19]. In Fig. 20, the results of the cast models for $b/D=2$ are shown together with those obtained from the cemented models. As is shown in this figure, the results obtained by the two tests are in excellent agreement over the all range of h/t examined. This fact shows that the method of cementation used in the present study is accurate satisfactorily and the effect of the cementation on the maximum stress at the hole boundary is not perceptible.

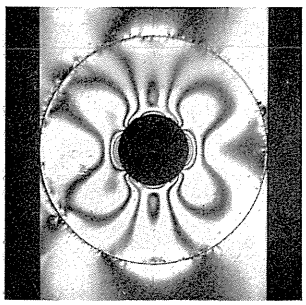

$K_1=1.61$

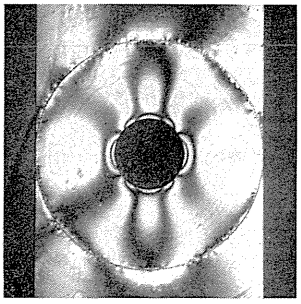

$K_2=1.74$

$b/D=1$, $h/t=1.91$, $d/D=0.3$, $r/t=0$

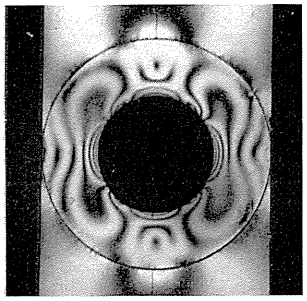

$K_1=1.52$

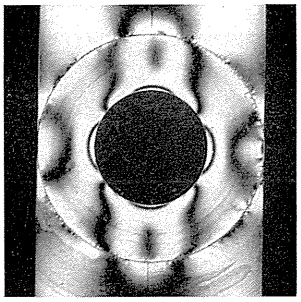

$K_2=1.76$

$b/D=1$, $h/t=2.92$, $d/D=0.5$, $r/t=0$

FIG. 23 (a). Dark-field frozen-stress patterns in rings ($b/D=1$).

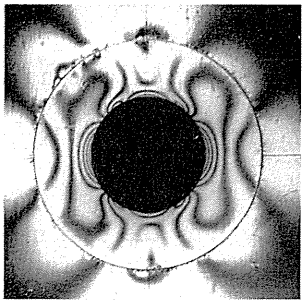

$K_1=2.01$

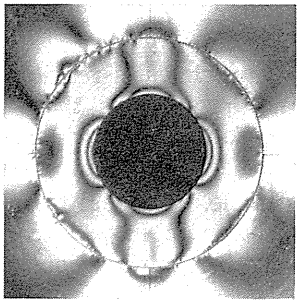

$K_2=2.15$

$b/D=2$, $h/t=1.98$, $d/D=0.5$, $r/t=0$

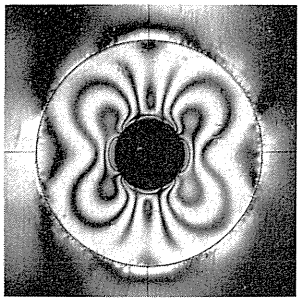

$K_1=1.22$

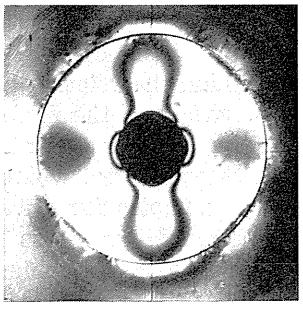

$K_2=1.61$

$b/D=2$, $h/t=2.95$, $d/D=0.3$, $r/t=0$

FIG. 23 (b). Dark-field frozen-stress patterns in rings ($b/D=2$).

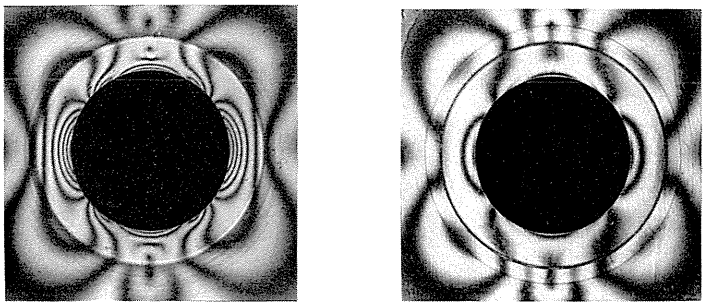

$K_1=1.64$ $K_2=1.96$

$b/D=2$, $h/t=3.04$, $d/D=0.7$, $r/t=1.67$

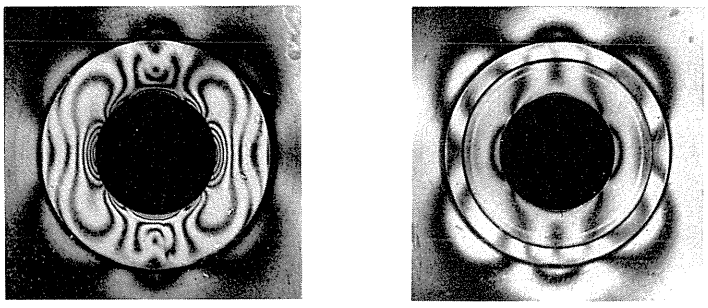

$K_1=1.03$ $K_2=1.63$

$b/D=2$, $h/t=4.91$, $d/D=0.5$, $r/t=0.83$

FIG. 23 (c). Dark-field frozen-stress patterns in rings ($b/D=2$).

From the experimental results herein obtained, it can be seen that the values of K_2 are much larger than those of K_1 with increase of h/t and the effective height of a reinforcing ring in the finite plate is three times as large as the plate thickness or somewhat larger.

As an example, dark-field frozen-stress patterns in the rings of different proportions are shown in Fig. 23 (a), (b) and (c). For the cast models, as was described in the foregoing, when the height of the ring was reduced to the plate thickness for the evaluation of the stress-concentration factor K_2, only the material around the hole was cut out from the ring, as is shown in figure (c), because the same model was used again to measure the stress concentration at the end of the fillet.

Since the limit of the effective height of the ring has been clarified, it is necessary to examine the relation between the stress-concentration factor K_2 and the radius of curvature of the fillet. Figures 24, 25, 26 and 27 show the stress-concentration factor K_2 for the models of $b/D=2$, plotted as a function of r/t. Broken lines in these figures, which are added for comparison, are the results of the preceding examples for a wide plate, namely, $b/D=4$. As is shown in these figures, the maximum stress herein obtained decreases with the increase of r/t, and this tendency is notable when $h/t>3$. Furthermore, it is seen from Figs. 26 and 27 that there is little difference between the results for $h/t=4$ and those for $h/t=5$ over the whole range of r/t examined. Hence, it may be said

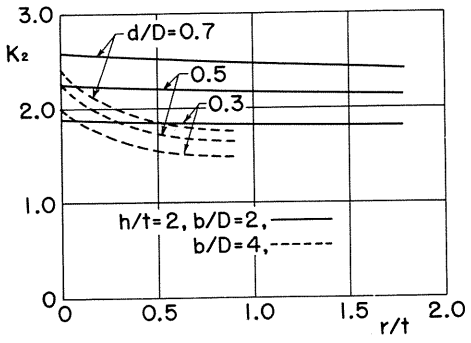

FIG. 24. Stress-concentration factor K_2 for $h/t=2$.

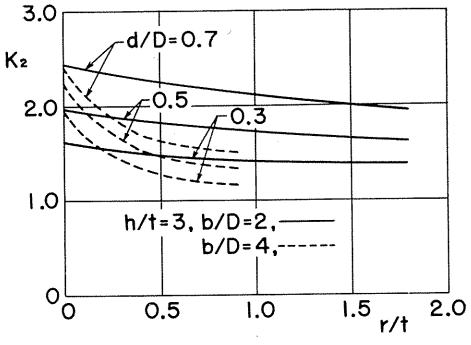

FIG. 25. Stress-concentration factor K_2 for $h/t=3$.

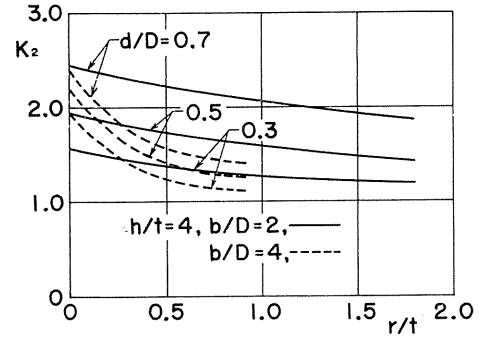

FIG. 26. Stress-concentration factor K_2 for $h/t=4$.

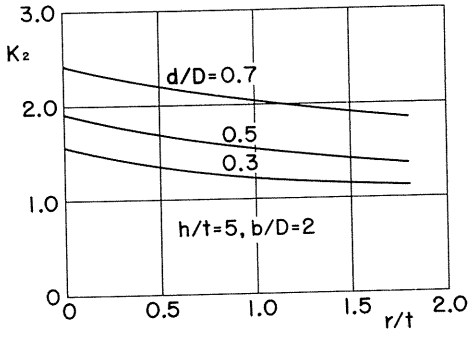

FIG. 27. Stress-concentration factcr K_2 for $h/t=5$.

that the effective limit of the ratio of the height of a ring to the plate thickness is three or somewhat larger, as was mentioned in the foregoing. The results for a wide plate show that the stress-concentration factors K_2 are reduced remarkably with increase of r/t. However, the rate of reduction of the factors K_2 for finite plates is not so intense as in the case of wide plates. This may be attributed to the effect of the edges of a finite plate on the maximum stress at the rim of a reinforced hole.

The stress concentrations at the ends of fillets were subsequently examined. As an example, dark-field frozen-stress patterns for the case of $h/t=4$ are shown in Fig. 28. The stress-concentration factor K_E at the location E (Fig. 3) for $h/t=4$, plotted as a function of r/t, is shown in Fig. 29. As shown in the figure, the factors K_E are considerably reduced with increase of r/t, and become almost constant for $r/t>1$. The similar tendency can be found in other cases of the height of rings, h/t, examined. This indicates that the effective limit of the radius of curvature of the fillet is equal to the plate thickness. As an example, if the dimensions of the ring are chosen as $h/t=4$ and $r/t=1$ for each wall thickness, the maximum stress at the rim of the hole is about 17 per cent smaller than that of the ring without fillets, as is shown in Fig. 26. It is noticeable that

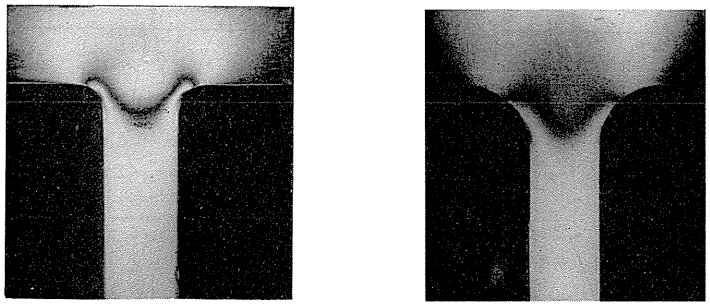

$K_E = 1.98$
$r/t = 0.33,\ d/D = 0.3$

$K_E = 1.51$
$r/t = 0.83,\ d/D = 0.3$

FIG. 28. Dark-field frozen-stress patterns at ends of fillets ($h/t = 4$).

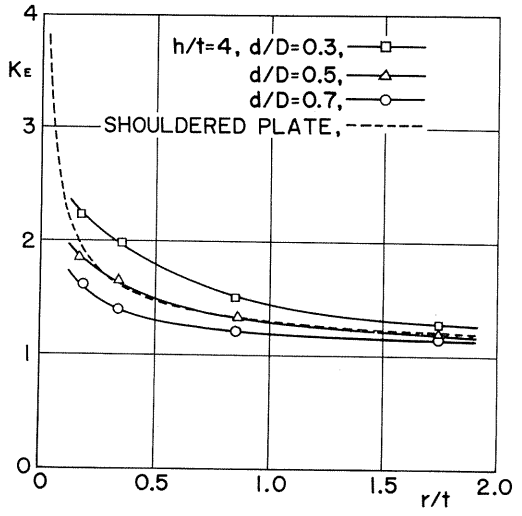

FIG. 29. Stress-concentration factor K_E for $h/t = 4$.

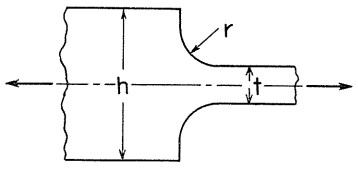

FIG. 30. Shouldered plate in tension ($h/t = 4$).

the factor K_E of the thick ring is larger than that of the thin ring. This is due to the fact that the rigidity of the thick ring is larger than that of the thin one. For comparison, the stress-concentration factor for a shouldered plate in tension (Fig. 30) is shown by a broken line in the same figure, which is calculated from Heywood's empirical formula[20] for $h/t = 4$. Comparing Fig. 29 with Fig. 26, it appears that if $r/t < 0.2$, the stress concentration at the end of the fillet is considerably larger than that at the edge of the reinforced hole.

Conclusions

The following conclusions are introduced from the photoelastic investigation for the symmetrical reinforcing ring around a central hole in a uniaxially loaded

plate:

1. The maximum stress at the rim of a reinforced hole, which is measured by slicing off the ring to the plate thickness, is much larger than that evaluated by the two-dimensional approach, with increase of the ratio of the ring height to the plate thickness, h/t. Moreover, the actual maximum stress occurs at the midpoint of the ring height and it is somewhat larger than the above-mentioned stress. Accordingly, the usual results predicted by the two-dimensional theoretical method are insufficient for design data of the reinforcement.

2. The effective height of the reinforcing ring for the reduction of the stress concentration at the rim of a reinforced hole is three times as large as the plate thickness. For the ring in a tension plate of finite width, however, it is more effective that the ratio h/t is somewhat larger than three.

3. For a wide plate, the maximum stress at the rim of a hole is markedly reduced by the use of a filleted ring in comparison with the use of a filletless ring, and the limit of the effective radius of curvature of the circular fillet is 0.6 times as large as the plate thickness. For a finite plate, however, the rate of reduction of the maximum stress due to the increase of fillet radius is not so intense as in the case of a wide plate, within the ratio of the fillet radius to the plate thickness examined.

4. From the results for the finite plate having the 2 : 1 ratio of the plate width to the ring diameter, the effective minimum of the radius of curvature of the fillet available in reducing the stress concentration at the ends of fillets is equal to the plate thickness. When the ratio of the fillet radius to the plate thickness is less than 0.2, the stress concentration at the corner of the fillet increases considerably as compared with that at the rim of the reinforced hole.

Acknowledgment

The author wishes to express his thanks to Professor Hajimu Ōkubo, Nagoya University, for his kind direction throughout the progress of the present investigation. The author also wishes to express his gratitude to Technical Official Yoshio Kurisu, Nagoya University, for his able assistance in performing the experiment.

References

1) M. Seika, M. Ishii and Y. Kurisu, Photoelastic Investigation of the Maximum Stress in an Infinite Plate with a Circular Hole Reinforced by a Stiffening Ring under Tension, Trans. Japan Soc. Mech. Eng., Vol. 29, No. 200, 1963, p. 745.

2) M. Seika, M. Ishii, K. Sakaki and Y. Kurisu, Photoelastic Investigation of the Maximum Stress in a Plate with a Reinforced Circular Hole under Tension, Trans. Japan Soc. Mech. Eng., Vol. 30, No. 212, 1964, p. 510.

3) M. Seika, M. Ishii and Y. Kurisu, Photoelastic Investigation of the Maximum Stress in a Plate with a Reinforced Circular Hole under Tension (Continued Report), Trans. Japan Soc. Mech. Eng., Vol. 30, No. 218, 1964, p. 1207.

4) M. Seika and M. Ishii, Photoelastic Investigation of the Maximum Stress in a Plate with a Reinforced Circular Hole Under Uniaxial Tension, J. Appl. Mech., Vol. 31, Trans. ASME, Vol. 86, 1964, p. 701.

5) M. Seika, A. Amano and Y. Kurisu, Photoelastic Investigation of the Maximum Stress in an Infinite Plate Having a Circular Hole Reinforced by a Stiffening Ring with Fillet under Tension, Trans. Japan Soc. Mech. Eng., Vol. 32, No. 243, 1966, p. 1647.

6) M. Seika and A. Amano, The Maximum Stress in a Wide Plate with a Reinforced Circular Hole Under Uniaxial Tension—Effects of a Boss with Fillet, J. Appl. Mech., Vol. 34, Trans. ASME, Vol. 89, 1967, p. 232.
7) M. Seika and M. Kojima, The Maximum Stress in a Plate with a Reinforced Circular Hole Under Uniaxial Tension—Effects of a Boss with Fillet, JSME 1967 Semi-International Symposium Papers, Experimental Mechanics, Vol. 1, 1967, p. 133.
8) C. Gurney, An Analysis of the Stresses in a Flat Plate with a Reinforced Circular Hole Under Edge Forces, Aeronau. Resear. Commit., R. and M., No. 1834, London, 1938.
9) L. Beskin, Strengthening of Circular Holes in Plates Under Edge Loads, J. Appl. Mech., Vol. 11, Trans. ASME, Vol. 66, 1944, p. A-140.
10) S. Levy, A. E. McPherson and F. C. Smith, Reinforcement of a Small Circular Hole in a Plane Sheet Under Tension, J. Appl. Mech., Vol. 15, Trans. ASME, Vol. 70, 1948, p. 160.
11) H. Reissner and M. Morduchow, Reinforced Circular Cutouts in Plane Sheets, NACA TN 1852, 1949.
12) J. R. M. Radok, Problems of Plane Elasticity for Reinforced Boundaries, J. Appl. Mech., Vol. 22, Trans. ASME, Vol. 77, 1955, p. 249.
13) G. N. Sawin, Spannungserhöhung am Rande von Löchern, VEB Verlag Technik, Berlin, 1956, S. 248.
14) O. Tamate, Stresses Around an Annular Inclusion in a Strip Under Tension, Trans. Japan Soc. Mech. Eng., Vol. 27, No. 173, 1961, p. 109.
15) A. Kaufman, P. T. Bizon and W. C. Morgan, Investigation of Circular Reinforcements of Rectangular Cross Section Around Central Holes in Flat Sheets Under Biaxial Loads in the Elastic Range, NASA TN D-1195, 1962.
16) S. Suzuki, Stress Measurements in a Plate Containing a Reinforced Circular Hole Using a Photoelastic Method, Intern. J. Mech. Sci., Vol. 6, 1964, p. 473.
17) S. Timoshenko and J. N. Goodier, Theory of Elasticity, McGraw-Hill Book Company, Inc., New York, 1951, p. 81.
18) R. C. J. Howland, On the Stresses in the Neighborhood of a Circular Hole in a Strip Under Tension, Phil. Trans. Roy. Soc., London, ser. A, Vol. 229, 1930, p. 49.
19) R. B. Heywood, Designing by Photoelasticity, Chapman and Hall, Ltd., London, 1952, p. 268.
20) R. B. Heywood, loc. cit., p. 178.